Chinese Journal of
POLYMER SCIENCE

RESEARCH ARTICLE

https://doi.org/10.1007/s10118-024-3100-1
Chinese J. Polym. Sci. **2024**, *42*, 907–915

Highly Transparent Fire-resistant Coatings with Intumescent Three-source Integration

Xiao-Liang Zeng[a], Xin-Sheng Lan[a], Yan Wang[a], Lin Zhang[b*], De-Ming Guo[b], and Hai-Bo Zhao[b*]

[a] *State Grid Sichuan Electric Power Research Institute, Chengdu 610041, China*
[b] *The Collaborative Innovation Center for Eco-Friendly and Fire-Safety Polymeric Materials (Ministry of Education), National Engineering Laboratory of Eco-Friendly Polymeric Materials (Sichuan), State Key Laboratory of Polymer Materials Engineering, College of Chemistry, Sichuan University, Chengdu 610064, China*

Electronic Supplementary Information

Abstract Wood, a readily available and sustainable natural resource, has found widespread use in construction and furniture. However, its inherent flammability poses a potential fire risk. Although intumescent fire-retardant coatings effectively mitigate this risk, achieving high transparency in such coatings presents a significant challenge. In our approach, we employed a cross-linked network of phytic acid anion and *N*-[3-(trimethoxysilyl) propyl]-*N*,*N*,*N*-trimethylammonium cation to create a transparent "three-in-one" intumescent coating. The collaborative P/N/Si flame-retardant effect markedly improved the intumescent char-forming capability, preventing the wood from rapid decomposition. This resulted in a substantial reduction in heat release (13.9% decrease in THR) and an increased limiting oxygen index (LOI) value of 35.5%. Crucially, the high transparency of the coating ensured minimal impact on the wood's appearance, allowing the natural wood grains to remain clearly visible. This innovative approach provides a straightforward method for developing transparent intumescent flame-retardant coatings suitable for wooden substrates. The potential applications extend to preserving ancient buildings and heritage conservation efforts.

Keywords Fire-resistant coating; Flame retardancy; Wood; Transparency

Citation: Zeng, X. L.; Lan, X. S.; Wang, Y.; Zhang, L.; Guo, D. M.; Zhao, H. B. Highly transparent fire-resistant coatings with intumescent three-source integration. *Chinese J. Polym. Sci.* **2024**, *42*, 907–915.

INTRODUCTION

Wood, a widely sourced renewable natural material, has historically been highly popular among building structural and furniture materials due to its easy processing, affordability, light weight, thermal insulation, and strong mechanical properties.[1–3] Wooden structures are particularly prevalent in ancient buildings and village houses.[4,5] However, the presence of lignin, cellulose, and hemicellulose, in addition to their porous structure, makes the wood highly flammable, posing a significant fire hazard.[6,7] The devastating fire at the Notre Dame Cathedral in Paris on April 15, 2019, resulted in the complete collapse of the wooden tower, causing serious social influence and enormous losses to the economy and culture.[8] China, a country with a long and rich history, has a large number of ancient wooden buildings that face potential fire risks. For reducing the damage caused by the fire, promoting fire-retardant technologies for wood-based materials is highly important.

* Corresponding authors, E-mail: 2022322030100@stu.scu.edu.cn (L.Z.)
E-mail: haibor7@163.com (H.B.Z.)

Special Issue: Functional Polymer Materials
Received December 31, 2023; Accepted February 26, 2024; Published online March 29, 2024

To date, tremendous efforts have been made to develop fire-resistant wood *via* the application of impregnated flame retardants[9,10] or surface flame-retardant coating treatments.[11–13] Li *et al.* reported that, through full-cell vacuum-pressure impregnation, flame retardant-treated wood exhibited a 47.7% reduction in total heat release (THR) and a limited oxygen index (LOI) of 41%.[14] Unfortunately, this particular treatment method requires high equipment requirements and applies only to unformed wood. In contrast, flame-retardant coatings are considered a relatively low-cost and highly efficient way to protect wooden materials, particularly in special fields such as historically significant buildings and precious furniture. For instance, Hao *et al.* developed a protective coating by combining waterborne polyurethane with commercially available flame retardants, each of which was approximately 250 μm in thickness.[15] This blend enhanced the fire resistance of the painted plywood, enabling it to withstand burning for approximately 20 min. Creating a fire-resistant layer for wood can be achieved effortlessly, without the need for complex pretreatment. The application of these coatings involves straightforward methods such as dipping, brushing, or spraying.[16–19] Importantly, the high flame-retardancy capabilities of an intumescent coating extend beyond wood and can be effectively applied to a diverse range of

substrates.

In the typical intumescent flame-retardant strategy, coatings are usually composed of an acid source (*e.g.*, ammonium polyphosphate), a gas source (*e.g.*, melamine), a carbon source (*e.g.*, pentaerythritol), and film-forming substances (*e.g.*, water-based acrylic resin, epoxy resin, amino resin).[20–22] When exposed to high-temperature fire or heat flux, the acid source will catalyze the dehydration of the carbon source and work together with the gas source to form a stable porous carbon foam on the surface.[23,24] This porous carbon shielding can block the transfer of heat and oxygen, effectively stopping or delaying flame spread, and protecting the substrate from fire damage.[25,26] However, because of the poor compatibility between intumescent flame retardants and film-forming substances, coatings generally exhibit low transparency. A transparent coating can preserve the natural beauty of wooden surfaces, making them highly desirable for heritage conservation. Opting for flame retardants with strong compatibility can enhance transparency but still does not prevent a decrease in flame retardant performance resulting from the migration of these agents to the surface over extended periods of use. By integrating the three intumescent sources, it is possible to achieve a highly transparent fire-retardant coating, but this has rarely been reported.

Herein, we propose a new eco-friendly strategy to develop a transparent and intumescent flame-retardant coating *via* the ionic interaction between a phytic acid anion and an *N*-[3-(trimethoxysilyl) propyl]-*N*,*N*,*N*-trimethylammonium cation cross-linked network. On one hand, the phosphorus-modified amino siloxane demonstrated the capability to swell, forming a synergistic flame-retardant carbon foam enriched with phosphorus, nitrogen, and silicon. This unique composition imparted wood with a notable LOI value of 35.5% while significantly reducing the total heat release (THR) by 13.9%. On the other hand, the integrated structure constructed by ionic bonds, combined with the exceptional film-forming properties of polysiloxane, enables the coating to maintain high transparency and minimally affects the appearance of the substrate. The simple construction process, highly effective intumescent flame retardancy performance, and optical transparency of these materials make this environmentally friendly coating a potential application for wooden materials, particularly on ancient buildings and precious furniture.

EXPERIMENTAL

Materials

Phytic acid sodium salt hydrate (PAS, with a purity over 90%) was obtained from Aladdin Chemicals Co., Ltd., (China). *N*-[3-(trimethoxysilyl)propyl]-*N*,*N*,*N*-trimethylammonium chloride (TMAPS, 50% in methanol) was obtained from Aladdin Chemicals Co., Ltd. (China).

Preparation of the Fire-resistant Coating and Treatment of Wood

Phytic acid sodium salt hydrate (20/10/0 g) was first dissolved in 200 g of deionized water, and the obtained solution was added to 40 g of *N*-[3-(trimethoxysilyl) propyl]-*N*,*N*,*N*-trimethylammonium chloride (50% in methanol) solution. Then, the mixture was heated to 60 °C for 8 h. The mass ratios of PAS:TMAPS were 2:2, 1:2, and 0:2, and the final coating solutions were conveniently written as P2N2, P1N2, and P0N2, respectively. The prepared coatings were treated by brushing onto wood, with a dry coating density of 500 g/m^2.

Characterization

Fourier transform infrared (FTIR) spectra were recorded by a Nicolet 6700 spectrometer in the frequency region of 4000–500 cm^{-1}. Scanning electron microscopy (SEM) images were obtained with a JSM-5900 L V scanning electron microscope at an acceleration voltage of 15 kV. The color difference was determined by using an NR10QC colorimeter (3nh Co., China). Thermogravimetric analysis (TGA) was carried out using a NETZSCH TG 209 F1 instrument at a heating rate of 10 °C/min under nitrogen atmospheres. The LOI values were measured on a JF-3 oxygen index tester (Jiangning Analytical Instrument Co., Ltd., China) with sample dimensions of 100 mm × 6.5 mm × 3 mm. The cabinet method was used to measure the weight loss and char index of the samples according to the Chinese standard GB12441-2018, and the weight loss and char index of the samples with dimensions of 300 mm × 150 mm × 5 mm were measured by an XSF-1-type fire resistant paint tester (small room mode) (Jiangning Analysis Instrument Co., China). The burning behavior of the 100 mm × 100 mm × 10 mm samples was measured by an FTT cone calorimeter at a heat flux of 50 kW/m^2. X-ray photoelectron spectroscopy (XPS) was performed with an X-ray photoelectron spectrometer (K-Alpha, Thermo Fisher Scientific Co., USA). Raman spectroscopy was carried out using a DXR2xi laser Raman spectrometer (Thermo Fisher Scientific Co., USA) with a 532 nm laser line.

RESULTS AND DISCUSSION

Fabrication and Characterization of the Coating

The construction of the transparent intumescent flame-retardant coating is illustrated in Fig. 1(a). Initially, ionic interactions between the phytic acid anion and the *N*-[3-(trimethoxysilyl) propyl]-*N*,*N*,*N*-trimethylammonium cation led to the formation of aggregates. Subsequently, a uniform polysiloxane cross-linked network was established *via* a facile sol-gel process. As shown in Fig. S1 (in the electronic supplementary information, ESI), the precursor liquids appear as pale-yellow transparent solutions with a noticeable Tyndall effect. According to the FTIR spectra (Fig. 1b and Fig. S2 in ESI), the absorption bands near 1125 (P=O) and 974 cm^{-1} (P—O)[27] can be observed in P2N2, as sodium ions were replaced by quaternary ammonium structures with higher electron cloud density, causing the bands to shift towards lower wavenumbers (1098 and 971 cm^{-1}).[28,29] In addition, the quaternary ammonium salt (—NR_3^+, 1478 cm^{-1}) shifted, indicating the successful introduction of PAS. The well-off construction of the Si—O—Si cross-linked network was also evident in the absorption bands[30] at 910 and 695 cm^{-1}. Furthermore, the more PAS was introduced, the more interaction sites were available. This was manifested by an increase in the size of the precursor liquid sol particles, as confirmed by Fig. 1(c). The above analysis results demonstrated that the coating was successfully prepared by ionic interactions and sol-gel processes.

The resulting coating displayed high optical transparency that is highly favorable for their applications. The characters

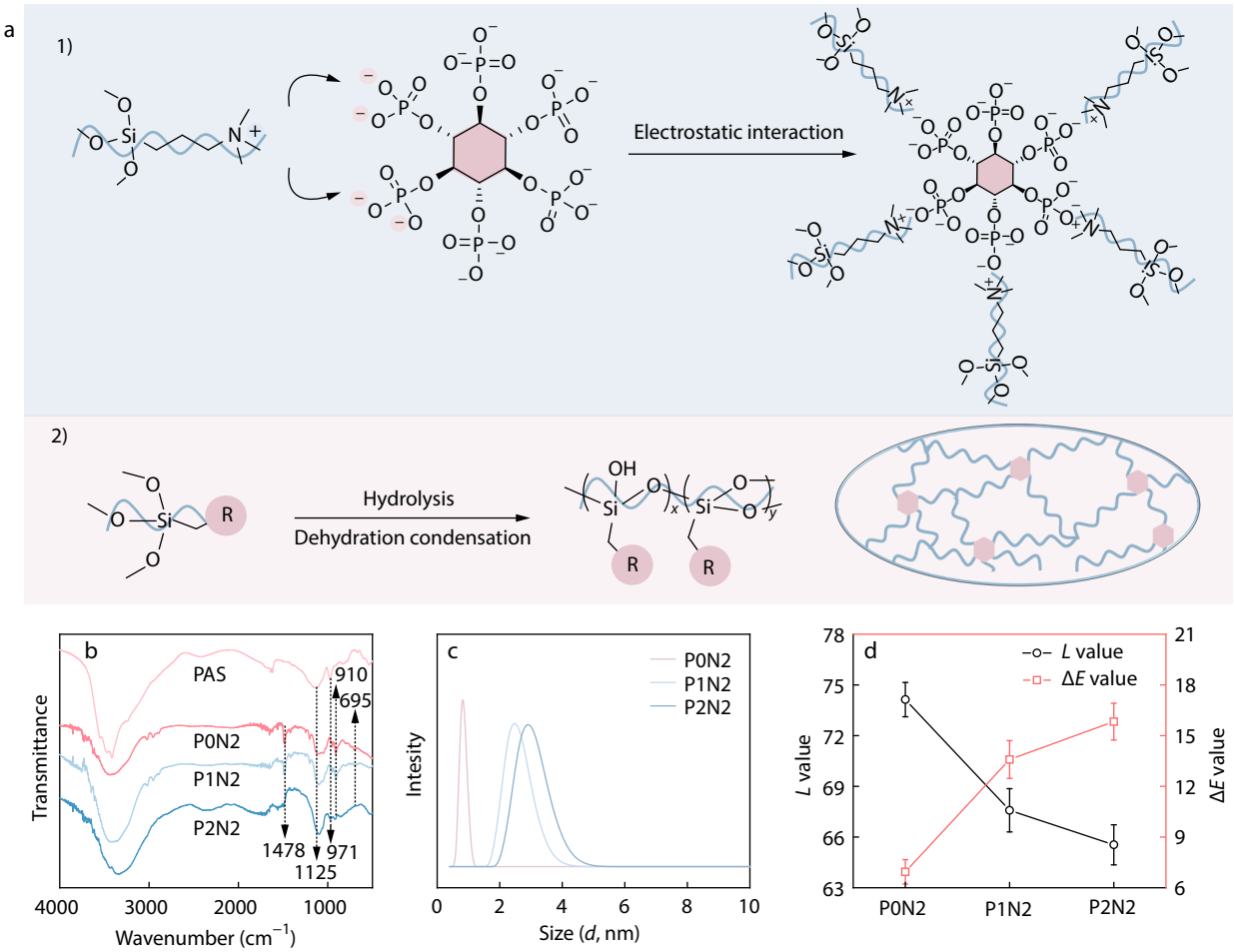

Fig. 1 (a) Schematic illustration of the preparation of the coating; (b) FTIR spectra of PAS, P0N2, P1N2, and P2N2; (c) Particle size distribution curves of precursor liquid for P0N2, P1N2, and P2N2; (d) Color changes of wood coated with P0N2, P1N2, and P2N2.

underneath the P2N2-coated glass were clearly visible (Fig. S3 in ESI), and the grains of the wood were completely undamaged after the P2N2 coating treatment, ensuring that the natural beauty of the wooden materials was preserved. The detailed influence of coating ratios on the color of the wooden substrates was investigated (Fig. 1d and Fig. S4 in ESI). As the PAS concentration increased, the *L* value, *i.e.*, the difference between light and dark, slightly decreased. And the Δ*E* value (color difference) increased, indicating that the flame-retardant coating treatment resulted in slight darkening and yellowing of the wood surface. However, a portion of the difference in color was due to the leaching of tannins from the wood by the water-based coating, and the use of a primer could help improve this phenomenon in the real applications.[31–33]

Thermal Stability and Flame-retardant Performance

The thermal stabilities of the PAS, P0N2, P1N2, and P2N2 coatings were investigated *via* TGA under a nitrogen atmosphere, and the experimental results are shown in Figs. 2(a) and 2(b) and Table 1. Without PAS, the P0N2 coating underwent two main thermal decomposition processes. The first one (290.6 ℃) was due to the cleavage of the alkyl N^+ bonds,[34,35] and the second one (489.9 ℃) was attributed to the further decomposition of the polysiloxane backbones. When added in low amounts of PAS, independent decomposition of PAS and P(TMAPS) dominated. Affected by the relatively high initial decomposition temperature ($T_{5\%}$, 220.2 ℃) and low maximum decomposition temperature (T_{max}, 217.4 and 306.2 ℃) of PAS, compared those to P0N2, $T_{5\%}$ of P1N2 increased by 24.0 ℃, T_{max1} decreased by 13.7 ℃, and T_{max2} had little changed, respectively. With the increasing addition of PAS, P2N2 exhibited significant decreases in $T_{5\%}$, T_{max1}, and T_{max2}, and the maximum thermal decomposition rate (R_{Tmax1}) sharply decreased by 77.0%. It is speculated that PAS and P(TMAPS) had strong synergistic effects. The char-forming capacities of the P1N2 and P2N2 coatings were markedly enhanced. The char residue at 700 ℃ increased significantly from 36.4 wt% for P0N2 to 46.2 wt% for P1N2 and 73.2 wt% for P2N2 respectively. The above results implied that, under the synergistic effect of P/N/Si, the dehydration and carbonization processes during decomposition largely accelerated, which was beneficial for the formation of a greater protective char layer and contributed to improving fire safety.

The flame-retardant performance of the coatings was evaluated first by the limiting oxygen index, defined as the minimum oxygen concentration (vol%)[36] needed to support the burning of materials. Fig. 2(c) illustrates that the LOI value of pristine wood was only 25.5% due to its highly flammable nature. After coating with P2N2, the LOI value of the material greatly increased by 39.2% from 25.5% to 35.5%, indicating

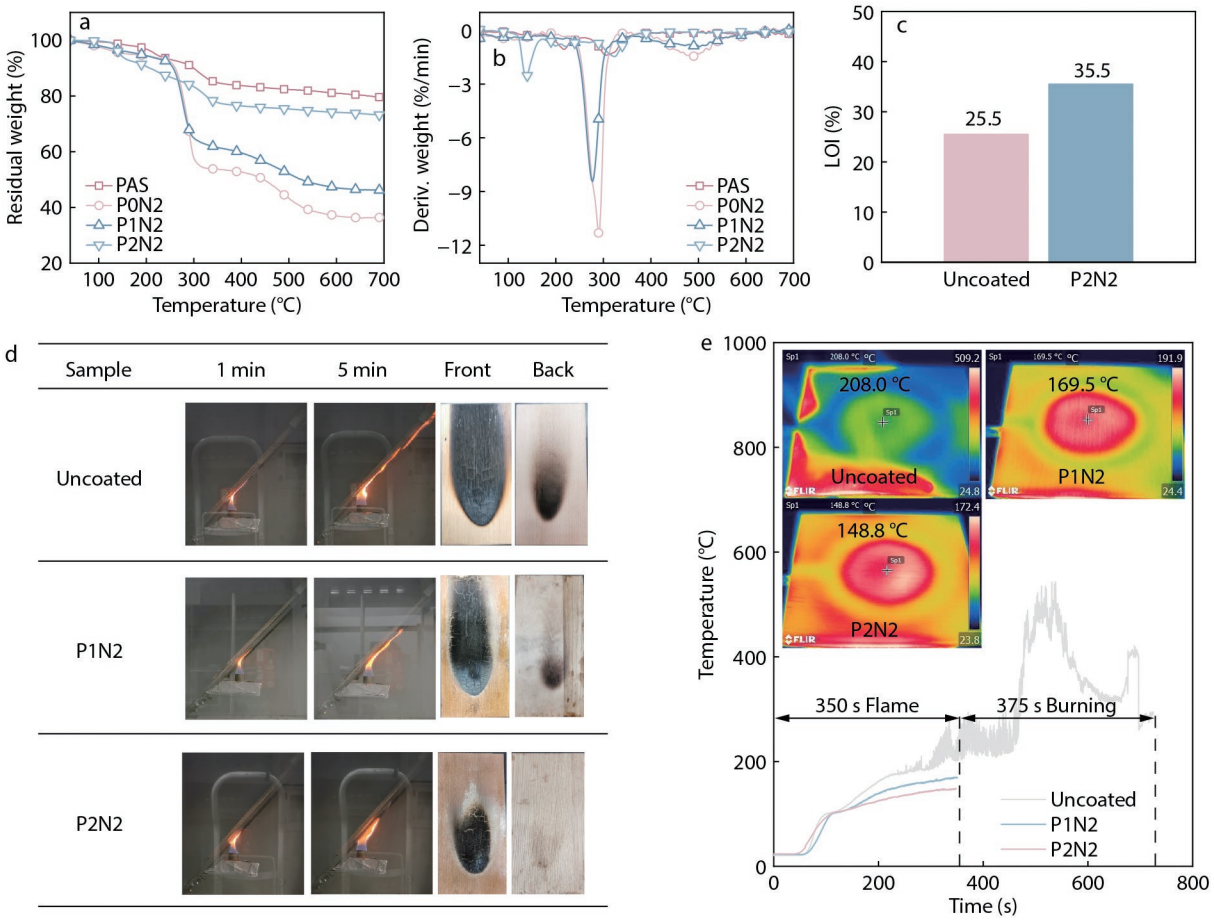

Fig. 2 (a) TG and (b) DTG curves of PAS, P0N2, P1N2 and P2N2; (c) LOI values of uncoated and P2N2 coated wood; (d) Digital photographs of uncoated, P1N2, and P2N2 coated wood in the cabinet test; (e) Time-dependent back-side temperature curves of uncoated wood, P1N2, and P2N2 coated wood burnt by alcohol flame.

Table 1 TGA data of the samples in a nitrogen atmosphere.

Sample	$T_{5\%}$ (°C)	T_{max1} (°C)	R_{Tmax1} (%/min)	T_{max2} (°C)	R_{Tmax2} (%/min)	C_{wt}^{700} (%)
PAS	220.2	217.4	−1.1	306.2	−13.9	79.5
P0N2	163.4	290.6	−11.3	489.9	−1.4	36.4
P1N2	187.4	276.9	−8.5	502.3	−0.9	46.2
P2N2	144.9	137.5	−2.6	323.4	−1.5	73.2

the excellent flame-retardant effect of the P/N/Si synergistic coating. This high LOI value denotes that the treated wood is difficult to ignite in a high oxygen concentration environment. The flame retardancy of wood is largely improved by the coating. In addition, the cabinet method[37] following the Chinese standard GB12441-2018 was used to assess the protective efficiency of the coating on the plywood. This evaluation primarily considered two parameters: mass loss and the char index. The results are listed in Fig. 2(d) and Table S1 (in ESI). It can be observed that the uncoated plywood was easily ignited, the flame spread rapidly upwards, and severe carbonization occurred on the burning surface. In contrast, under the protection of the P1N2 or P2N2 coating, the flame spread was greatly suppressed, especially for P2N2. The intumescent char layer blocked the fire and heat from eroding the substrate. Compared with uncoated plywood, the back of the P1N2 coated has lighter burn mark, and there was no burn mark on the back of the P2N2 coated. The uncoated plywood shows high mass loss (25.0 g) and a high char index (154.0 cm^3). In the case of the P1N2-coated plywood, there is a significant reduction in both the mass loss and char index, with values decreasing to 12.4 g and 126.9 cm^3, respectively. Furthermore, the P2N2 coating on the plywood yielded the most effective enhancement in fire resistance, resulting in a remarkable 76.4% reduction in mass loss and a substantial 74.6% reduction in the char index. Furthermore, as shown in Fig. S5 (in ESI) and Fig. 2(e), the plywood was burned with an alcohol flame (~500 °C) and the temperature change of its back-side was detected with an infrared thermography instrument. The alcohol fuel could burn for ~350 s, and the back-side temperature of the uncoated plywood continued to rise during the burning, reaching 208.0 °C. Due to being ignited by flame, after no alcohol, it still sustained burning for another 375 s before dying out, and the highest temperature

https://doi.org/10.1007/s10118-024-3100-1

reached 545.5 °C. The back-side temperatures rise rate of P1N2 and P2N2 coated plywood significantly slowed, and the highest temperatures within 350 s were 169.5 and 148.8 °C, respectively. More importantly, benefiting by the formation of dense char layers on the surface, P1N2 and P2N2 coated plywood achieved self-extinguishing immediately after alcohol burnout. These results substantiated the hypothesis proposed above that a synergistic effect occurred at high phosphorus contents, resulting in the formation of a thicker and more stable char layer, which further protected the substrate from burning and heat radiation.

A cone calorimetry test,[38] an oxygen consumption technique providing a burning scenario similar to that of a real fire, was used to further investigate the heat and smoke release of coated wood. The peak heat release rate (PHRR), total heat release (THR), total smoke release (TSR), and residues after the test are summarized in Table S2 (in ESI), and the corresponding curves of HRR, THR and TSR are shown in Figs. 3(a)–3(c). After ignition for 3 s, the HRR values of the untreated wood increased rapidly, reaching the first peak value of 291.1 kW/m^2 in a short time of 40 s. Subsequently, the HRR value reached a second peak value of 297.1 kW/m^2 within another 185 s. This burning behavior represented a characteristic charring phenomenon of materials during combustion. The first HRR peak was attributed to the initial pyrolysis of wood, the subsequent decrease in the HRR was attributed to the formation of a char layer, and the cracking of the char layer caused the emergence of a second peak. After coated by P0N2 and P1N2, the wood exhibited a similar two-stage heat release behavior. Although the P0N2 coating helped wood reduce PHRR1 to 210.4 kW/m^2, the large amount of flammable alkyl chains in the coating resulted in a rise in PHHR2 to 317.4 kW/m^2. Under the protection of the P1N2 coating, both PHRR1 and RHRR2 decreased by 29.7% and 7.6%, respectively. Notably, the P2N2 coating broke the dilemma of char layer rupture, delaying the time to arrive the peak heat release by 230 s, and only one PHRR value of 269.3 kW/m^2 was observed. Moreover, compared to those of untreated wood, THR and TSR of P2N2-coated wood slightly decreased from 68.9 MJ/m^2 and 1281.1 m^2/m^2 to 59.3 MJ/m^2 and 1214.1 m^2/m^2, respectively. A much gentler slope in the THR and TSR curves of P2N2 indicated that a more stable char layer could slow the release of heat and smoke. In addition, FIGRA (fire growth rate = maximum quotient of HRR(t)/t)[39] was calculated to assess the hazard of developing fires. The larger the FIGRA index is, the faster the combustion growth and the higher the fire risk. The P2N2 treated wood, with a minimum value of 2.4 kW/m^2, was the safest and able to reduce fire damage.

Flame-retardant Mechanism

Generally, intumescent flame-retardant coatings work simulta-

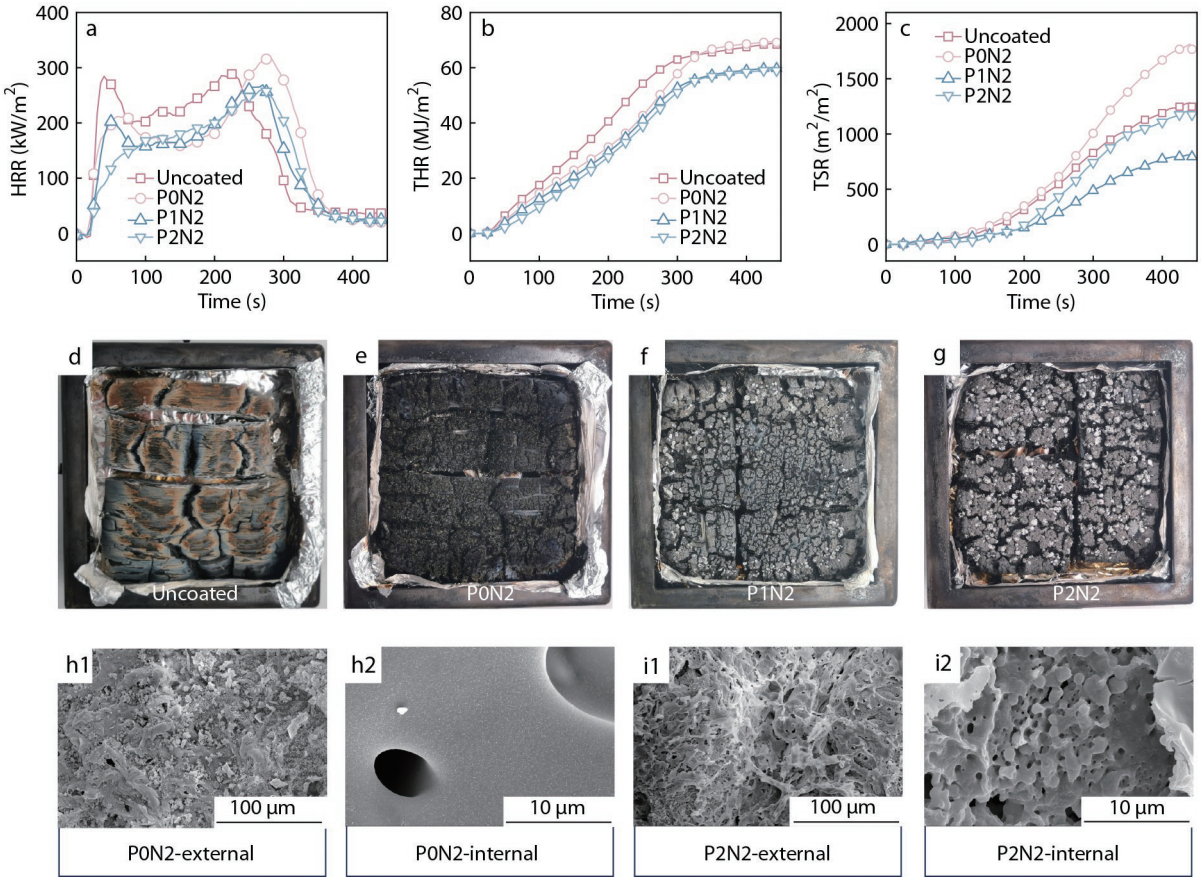

Fig. 3 (a) Heat release rate (HRR), (b) total heat release (THR), and (c) total smoke release (TSR) curves. Characterization of the residual char after the cone calorimetry test: digital pictures of (d) uncoated, (e) P0N2-coated, (f) P1N2-coated, and (g) P2N2-coated wood; SEM images of (h1 and h2) P0N2 and (i1 and i2) P2N2 coatings.

https://doi.org/10.1007/s10118-024-3100-1

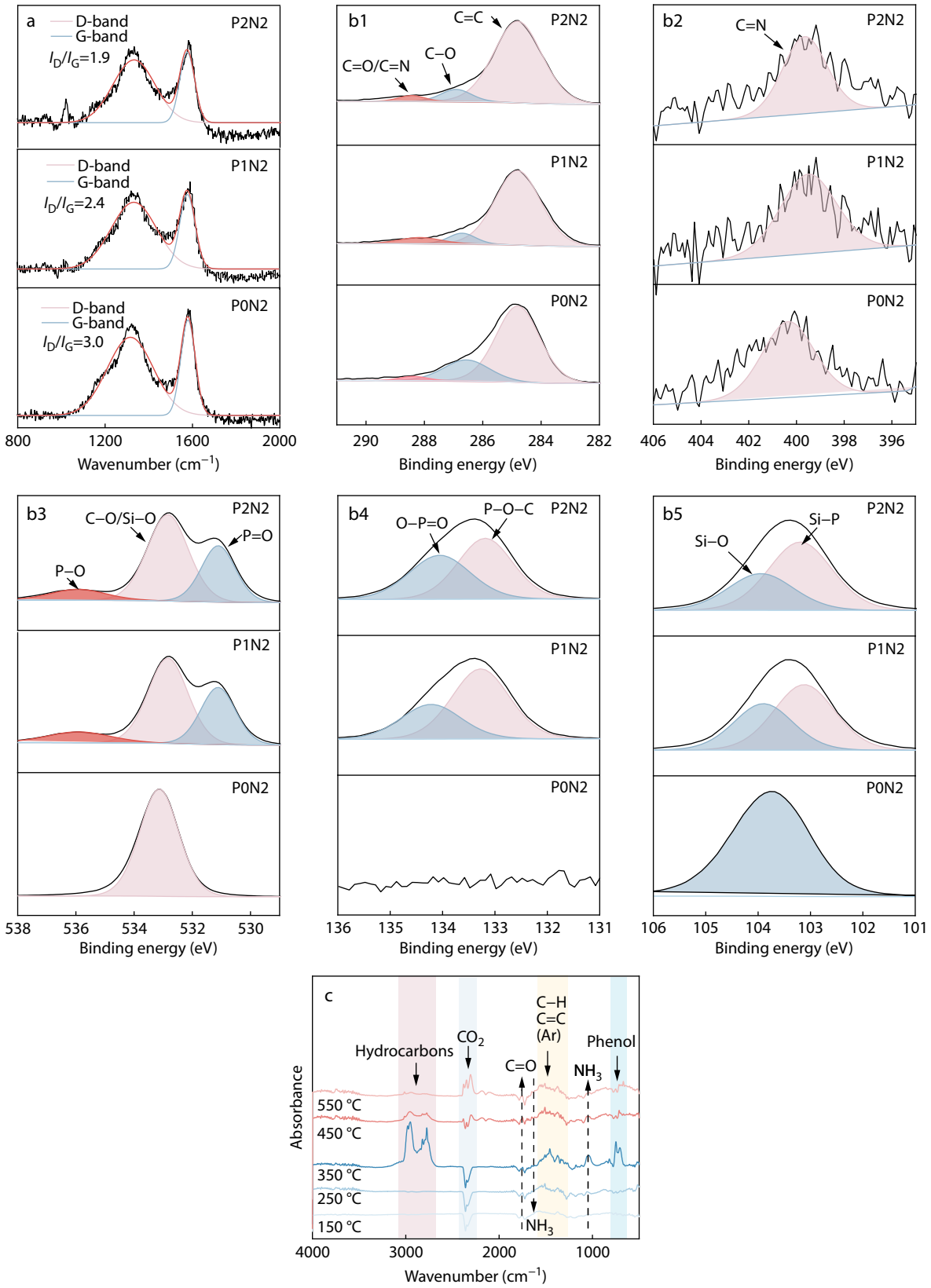

Fig. 4 (a) Raman spectra of coating char residues for P0N2, P1N2, and P2N2; XPS spectra of coating char residues for P0N2, P1N2, and P2N2: binding energies of (b1) C_{1S}, (b2) N_{1s}, (b3) O_{1s}, (b4) P_{2P}, and (b5) Si_{2P}; (c) TG-IR curves of the P2N2 coating.

https://doi.org/10.1007/s10118-024-3100-1

neously in both the gas and condensed phases. First, to understand the flame-retardant mechanism in the condensed phases of the coatings, the residual char after the cone calorimeter test was investigated in detail. As shown in Figs. 2(d)–2(g), the burnt wood left only a small amount of loose carbon (yield 13.8%), while after coating, darker and stronger char layers were evident on the surface. In particular, the P2N2 coating formed abundant white expanded char particles, with a high char residue of 20.0%. Furthermore, the SEM images (Figs. 3h1–3h2) of residues from the P0N2 coating revealed a tightly stacked char layer with a smooth interior, indicating a non-intumescent behavior. In contrast, the residue of the P2N2 coating exhibited the typical characteristics of an intumescent char, with a porous honeycomb-like structure inside due to the release of gas. This suggests that PAS not only acted as an acid source but also as a gas source. Raman spectroscopy was used to further investigate the different forms of carbon in the residual char, and the bands at 1360 cm^{-1} (D band) and 1580 cm^{-1} (G band) corresponded to the disordered graphitic structure and graphitic structure,[40,41] respectively. It is generally considered that the intensity ratio of I_D/I_G is inversely proportional to the graphitization degree,[42] for which a smaller I_D/I_G ratio indicates a greater graphitization degree and more stable char. Compared with the I_D/I_G values of the P0N2 coating, the values of P1N2 and P2N2 were reduced by 0.6 and 1.1, respectively (Fig. 4a), demonstrating more compact and more thermally stable chars. To ascertain the chemical elements and structures in the char residues, X-ray photoelectron spectroscopy (XPS) was carried out, and the results are illustrated in Figs. 4(b1)–4(b5) and Table S3 (in ESI). The residues were mainly composed of C, O, Si elements, with the addition of P in P1N2 and P2N2. This plentiful phosphorus residue in the condensed phase plays a vital role. However, only trace amounts of N element remained, which was difficult to monitor and might be released as gases. The C_{1s} curves exhibited three distinct peaks: 288.4 eV (C═O/C═N), 286.8 eV (C—O),[43] and 284.8 (C═C). In the N_{1s} spectra, the binding energy at 400.0 eV was attributed to C═N.[44] Two new peaks at 535.8 eV (P—O) and 531.2 eV (P═O)[45] appeared in the O_{1s} spectra of P1N2 and P2N2, and the peak at 532.9 eV was attributed to C—O/Si—O. The P_{2p} spectra could be deconvoluted to P—O—C (133.2 eV) and O—P═O (134.2 eV).[44] The peaks at 103.8 eV and 103.0 eV in the Si_{2p} spectra verified the presence of Si—O and Si—P, respectively, and the formation of silica further enhanced the strength of the char layer. The above results illustrated that the coating facilitated the formation of C═C, C═N, P—O—C, P═O, and Si—O bonds, which play prominent roles in condensing phase flame retardants.

Furthermore, the gaseous thermal decomposition products of the P2N2 coating were investigated by using thermogravimetric analysis-infrared spectrometry (TG-IR), as shown in Fig. 4(c). The strongest signal of gas-phase products emerged at approximately 350 °C, corresponding to the second peak temperature of thermal decomposition in the DTG analysis. The gas phase products mainly comprised hydrocarbons (2946 cm^{-1}),[46,47] CO_2 (2360 cm^{-1}),[48] NH_3 (1040, 1630 cm^{-1}),[14] and aromatic compounds (1455, 751 cm^{-1}).[49] As shown in Fig. S6 (in ESI), the peak intensity of NH_3 dramatically increased with increasing temperature from 300 °C to 350 °C, and CO_2 was released at a constant rate. The release of a large amount of non-flammable gases could attenuate the concentration of combustive supporting gases, thus effectively preventing flame spread.

Based on the above analysis, a possible intumescent flame-retardant mechanism was proposed, as shown in Fig. 5. When exposed to fire, incipiently, the quaternary ammonium structure detached from the polysiloxane chain, and the phytic acid anion decomposed into smaller phosphoric acid structures. As the temperature further increased, the partial quaternary ammonium underwent thermal decomposition, releasing CO_2 and NH_3 gases, while the residue remained in the char. In addition, the main chain of polysiloxane was broken, and some oligosiloxanes and silica were produced. Meanwhile, phosphoric acid formed polyphosphoric acid through dehydration to participate in forming char, and promoted dehydration and carbonization of other carbon sources, jointly constructing high-strength and stable phosphorus, nitrogen, and silicon hybrid cross-linked aromatic pyridinic char layer. During this process, the massive release of non-flammable gases not only diluted the fuel concentration in the combustion zone, effectively slowing the combustion, but also played an important role in puffing char layer. This intumescent hybrid char layer functioned as a robust physical barrier, inhibiting the transfer of oxygen and heat while preventing the release of combustible gases. Consequently, this material exhibited high-efficiency flame-retardant performance.

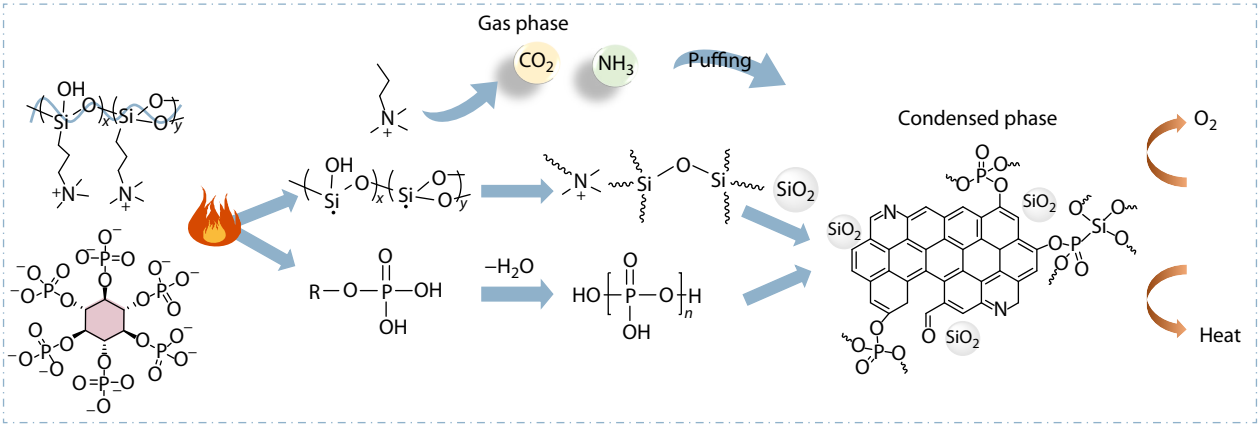

Fig. 5 Proposed intumescent flame-retardant mechanism of the P2N2 coating.

https://doi.org/10.1007/s10118-024-3100-1

CONCLUSIONS

To summarize, an eco-friendly transparent intumescent flame-retardant coating was successfully prepared *via* ionic interactions between a phytic acid anion and an *N*-[3-(trimethoxysilyl) propyl]-*N*,*N*,*N*-trimethylammonium cation. The homogeneous "three sources in one" protective coating had high optical transparency, resulting in little apparent effect on the substrate. Owing to the P/N/Si intumescent hybrid char layer, the coating effectively blocked the erosion of fire and heat to the wood substrate. P2N2-coated wood achieved efficient flame-retardant performance with a high LOI value of 35.5%, a 76.4% reduction in mass loss, and a 13.9% decrease in the THR. Because of the good transparency and high efficiency of flame retardants in coatings, these coatings have great potential for protecting villages with minority characteristics, ancient buildings, and other heritage sites.

Conflict of Interests

The authors declare no interest conflict.

Electronic Supplementary Information

Electronic supplementary information (ESI) is available free of charge in the online version of this article at http://doi.org/10.1007/s10118-024-3100-1.

Data Availability Statement

The data that support the findings of this study are available from the corresponding author upon reasonable request. The authors' contact information: 2022322030100@stu.scu.edu.cn (L.Z.), haibor7@163.com (H.B.Z.)

ACKNOWLEDGMENTS

This work was financially supported by State Grid Corporation of China Science and Technology Project Funding (No. 52199723000M), the National Natural Science Foundation of China (No. 52122302) and Sichuan Science and Technology Program (No. 2023NSFSC1943).

REFERENCES

1 Zhang, M. F.; Wang, D.; Li, T.; Jiang, J.; Bai, H. Y.; Wang, S. B.; Wang, Y.; Dong, W. F. Multifunctional flame-retardant, thermal insulation, and antimicrobial wood-based composites. *Biomacromolecules* **2023**, *24*, 957–966.
2 Kolibaba, T. J.; Vest, N. A.; Grunlan, J. C. Polyelectrolyte photopolymer complexes for flame retardant wood. *Mater. Chem. Front.* **2022**, *6*, 1630–1636.
3 Zhao, X. J.; Liang, Z. W.; Huang, Y. B.; Hai, Y.; Zhong, X. D.; Xiao, S.; Jiang, S. H. Influence of phytic acid on flame retardancy and adhesion performance enhancement of poly(vinyl alcohol) hydrogel coating to wood substrate. *Prog. Org. Coatings* **2021**, *161*, 106453.
4 Yi, L.; Yang, Q.; Yan, L.; Wang, N. A facile strategy to construct ZnO nanoparticles reinforced transparent fire-retardant coatings for achieving antibacterial activity and long-term fire protection of wood substrates. *J. Building Eng.* **2023**, *72*, 106630.
5 Wang, K. H.; Wang, S. H.; Meng, D.; Chen, D.; Mu, C. Z.; Li, H. F.; Sun, J.; Gu, X. Y.; Zhang, S. A facile preparation of environmentally-benign and flame-retardant coating on wood by comprising polysilicate and boric acid. *Cellulose* **2021**, *28*, 11551–11566.
6 Zhong, J.; Huang, Y. S.; Chen, Y. T.; Li, L. P.; Guo, C. G. Synthesis of eugenol-modified epoxy resin and application on wood flame retardant coating. *Indust. Crops Products* **2022**, *183*, 114979.
7 Lu, J. H.; Jiang, P.; Chen, Z. L.; Li, L. M.; Huang, Y. X. Flame retardancy, thermal stability, and hygroscopicity of wood materials modified with melamine and amino trimethylene phosphonic acid. *Constr. Building Mater.* **2021**, *267*, 121042.
8 Barthélemy, J. Avoiding predictable surprises: lessons from the fire at Notre Dame de Paris. *Organizational Dynamics* **2023**, *52*, 100966.
9 Song, K. L.; Ganguly, I.; Eastin, I.; Dichiara, A. High temperature and fire behavior of hydrothermally modified wood impregnated with carbon nanomaterials. *J. Hazard. Mater.* **2020**, *384*, 121283.
10 Yan, D.; Chen, D.; Tan, J.; Yuan, L. P.; Huang, Z. Z.; Zou, D. F.; Sun, P. H.; Tao, Q.; Deng, J. Y.; Hu, Y. C., Synergistic flame retardant effect of a new N-P flame retardant on poplar wood density board. *Polym. Degrad. Stabil.* **2023,** *211*, 110331.
11 Sykam, K.; Hussain, S. S.; Sivanandan, S.; Narayan, R.; Basak, P. Non-halogenated UV-curable flame retardants for wood coating applications: review. *Prog. Org. Coatings* **2023**, *179*, 107549.
12 Puyadena, M.; Etxeberria, I.; Martin, L.; Mugica, A.; Agirre, A.; Cobos, M.; Gonzalez, A.; Barrio, A.; Irusta, L. Polyurethane/acrylic hybrid dispersions containing phosphorus reactive flame retardants as transparent coatings for wood. *Prog. Org. Coatings* **2022**, *170*, 107005.
13 Zhang, J. Y.; Zeng, F. R.; Liu, B. W.; Wang, Z. H.; Lin, X. C.; Zhao, H. B.; Wang, Y. Z. A biomimetic closed-loop recyclable, long-term durable, extreme-condition resistant, flame-retardant nanocoating synthesized by reversible flocculation assembly. *Mater. Horiz.* **2023**, *10*, 4551–4561.
14 Li, L. M.; Chen, Z. L.; Lu, J. H.; Wei, M.; Huang, Y. X.; Jiang, P. Combustion behavior and thermal degradation properties of wood impregnated with intumescent biomass flame retardants: phytic acid, hydrolyzed collagen, and glycerol. *ACS Omega* **2021**, *6*, 3921–3930.
15 Hao, W. T.; Zheng, Q. N.; Zhong, Y. N. J.; Meng, X. K.; Wang, H. L.; Qiu, L. Z.; Lu, H. B.; Huang, Y. P.; Yang, W. An eco-friendly and facile method to prepare waterborne polyurethane based fire-resistant & waterproof coatings for wood protection. *Prog. Org. Coatings* **2023**, *185*, 107892.
16 Chen, M. X.; Dai, J. Y.; Zhang, L. Y.; Wang, S. P.; Liu, J. K.; Wu, Y. G.; Ba, X. W.; Liu, X. Q. The role of renewable protocatechol acid in epoxy coating modification: significantly improved antibacterial and adhesive properties. *Chinese J. Polym. Sci.* **2024**, *42*, 63–72.
17 Li, C. B.; Wang, F.; Sun, R. Y.; Nie, W. C.; Song, F.; Wang, Y. Z. A multifunctional coating towards superhydrophobicity, flame retardancy and antibacterial performances. *Chem. Eng. J.* **2022**, *450*, 138031.
18 Wang, Z. H.; Liu, B. W.; Zeng, F. R.; Lin, X. C.; Zhang, J. Y.; Wang, X. L.; Wang, Y. Z.; Zhao, H. B. Fully recyclable multifunctional adhesive with high durability, transparency, flame retardancy, and harsh-environment resistance. *Sci. Adv.* **2022**, *8*, eadd8527.
19 Zhang, Y. L.; Ma, Z. L.; Ruan, K. P.; Gu, J. W. Multifunctional $Ti_3C_2T_x$-(Fe_3O_4/polyimide) composite films with Janus structure for outstanding electromagnetic interference shielding and superior visual thermal management. *Nano Res.* **2022**, *15*, 5601–5609.
20 Wang, T.; Long, M. C.; Zhao, H. B.; An, W. L.; Xu, S. M.; Deng, C.;

Wang, Y. Z. Temperature-responsive intumescent chemistry toward fire resistance and super thermal insulation under extremely harsh conditions. *Chem. Mater.* **2021**, *33*, 6018–6028.
21 Tian, Y. C.; Wang, C. Y.; Ai, Y. F.; Tang, L. C.; Cao, K. Phytate-based transparent and waterproof intumescent flame-retardant coating for protection of wood. *Mater. Chem. Phys.* **2023**, *294*, 127000.
22 Yan, L.; Xu, Z. S.; Liu, D. L. Synthesis and application of novel magnesium phosphate ester flame retardants for transparent intumescent fire-retardant coatings applied on wood substrates. *Prog. Org. Coatings* **2019**, *129*, 327–337.
23 Zhang, L.; Zheng, G. Q.; Chen, X. L.; Guo, S. Q.; Zeng, F. R.; Liu, B. W.; Zeng, X. L.; Lan, X. S.; Wang, Y. Z.; Zhao, H. B. Smart self-puffing phosphite-protonated siloxane network enables multifunctional transparent protection. *ACS Mater. Lett.* **2023**, *5*, 2398–2407.
24 Wang, Y. C.; Zhao, J. P. Benign design of intumescent flame retardant coating incorporated various carbon sources. *Constr. Building Mater.* **2020**, *236*, 117433.
25 Jin, W. J.; He, W. L.; Gu, L.; Cheng, X. W.; Guan, J. P. An eco-friendly and intumescent P/N/S-containing flame retardant coating for polyamide 6 fabric. *Eur. Polym. J.* **2022**, *180*, 111610.
26 Liu, B. W.; Zhao, H. B.; Wang, Y. Z. Advanced flame-retardant methods for polymeric materials. *Adv. Mater.* **2022**, *34*, e2107905.
27 Yang, J. Y.; Xia, Y.; Zhao, J.; Yi, L. F.; Song, Y. J.; Wu, H.; Guo, S. Y.; Zhao, L. J.; Wu, J. R. Flame-retardant and self-healing biomass aerogels based on electrostatic assembly. *Chinese J. Polym. Sci.* **2020**, *38*, 1294–1304.
28 Bui, H. L.; Huang, C. J. Tough polyelectrolyte hydrogels with antimicrobial property via incorporation of natural multivalent phytic acid. *Polymers* **2019**, *11*, 1721.
29 Zhang, T.; Yan, H. Q.; Shen, L.; Fang, Z. P.; Zhang, X. M.; Wang, J. J.; Zhang, B. Y. Chitosan/phytic acid polyelectrolyte complex: a green and renewable intumescent flame retardant system for ethylene-vinyl acetate copolymer. *Industr. Engin. Chem. Res.* **2014**, *53*, 19199–19207.
30 Huang, H.; Wu, C.; Wu, S. Q.; Pan, R. Q.; Yin, L. H.; Jin, X. Y.; Pan, Y. W.; Wang, H. B.; Yan, X. J.; Hong, C. Q.; Han, W. B.; Zhang, X. H. Super-flexible, thermostable and superhydrophobic polyimide/silicone interpenetrating aerogels for conformal thermal insulating and strain sensing applications. *Chem. Eng. J.* **2022**, *441*, 136032.
31 Suttie, E.; Ekstedt, J. Evaluation of a method to determine discoloration of paints on wood due to tannin staining from knots. *Surface Coatings Inter. Part B: Coatings Transactions* **2004**, *87*, 57–61.
32 Yalcin, M.; Pelit, H.; Akcay, C.; Cakicier, N. Surface properties of tannin-impregnated and varnished beech wood after exposure to accelerated weathering. *Coloration Technol.* **2017**, *133*, 334–340.
33 Coniglio, R.; Gaschler, W.; Clavijo, L. Water-based system to prevent the yellowing of opaque coatings on knotted pine wood. *J. Coatings Technol. Res.* **2023**, *20*, 781–788.
34 Borodina, E.; Karpov, S. I.; Selemenev, V. F.; Schwieger, W.; Maracke, S.; Fröba, M.; Rößner, F. Surface and texture properties of mesoporous silica materials modified by silicon-organic compounds containing quaternary amino groups for their application in base-catalyzed reactions. *Microporous Mesoporous Mater.* **2015**, *203*, 224–231.
35 Wang, L. Y.; Li, L. S.; Fan, Q. H.; Chu, T. X.; Wang, Y.; Xu, Y. L. Thermal stability and flammability of several quaternary ammonium ionic liquids. *J. Molecular Liquids* **2023**, *382*, 121920.
36 Zhang, L.; Liu, B. W.; Wang, Y. Z.; Fu, T.; Zhao, H. B. P-doped PANI/AgMWs nano/micro coating towards high-efficiency flame retardancy and electromagnetic interference shielding. *Compos. Part B Eng.* **2022**, *238*, 109944.
37 Sun, R. Y.; Wang, F.; Li, C. B.; Deng, Z. P.; Song, F.; Wang, Y. Z. Formulation of environmentally robust flame-retardant and superhydrophobic coatings for wood materials. *Constr. Building Mater.* **2023**, *392*, 131873.
38 Schartel, B.; Hull, T. R. Development of fire-retarded materials—interpretation of cone calorimeter data. *Fire Mater.* **2007**, *31*, 327–354.
39 Shi, X. H.; Chen, L.; Liu, B. W.; Long, J. W.; Xu, Y. J.; Wang, Y. Z. Carbon fibers decorated by polyelectrolyte complexes toward their epoxy resin composites with high fire safety. *Chinese J. Polym. Sci.* **2018**, *36*, 1375–1384.
40 Liu, Z.; Fan, X. L.; Zhang, J. L.; Chen, L. X.; Tang, Y. S.; Kong, J.; Gu, J. W. PBO fibers/fluorine-containing liquid crystal compound modified cyanate ester wave-transparent laminated composites with excellent mechanical and flame retardance properties. *J. Mater. Sci. Technol.* **2023**, *152*, 16–29.
41 Wu, T.; Yang, F. H.; Tao, J.; Zhao, H. B.; Yu, C. B.; Rao, W. H. Design of P-decorated POSS towards flame-retardant, mechanically-strong, tough and transparent epoxy resins. *J. Colloid Interface Sci.* **2023**, *640*, 864–876.
42 Wei, C. X.; Gao, T. Y.; Xu, Y.; Yang, W. J.; Dai, G. J.; Li, R.; Zhu, S. E.; Yuen, R. K. K.; Yang, W.; Lu, H. D. Synthesis of bio-based epoxy containing phosphine oxide as a reactive additive toward highly toughened and fire-retarded epoxy resins. *Chinese J. Polym. Sci.* **2023**, *41*, 1733–1746.
43 Xie, H. L.; Lai, X. J.; Li, H. Q.; Gao, J. F.; Zeng, X. R.; Huang, X. Y.; Lin, X. Y. A highly efficient flame retardant nacre-inspired nanocoating with ultrasensitive fire-warning and self-healing capabilities. *Chem. Eng. J.* **2019**, *369*, 8–17.
44 Fu, C.; Ye, W.; Zhai, Z. J.; Zhang, J.; Li, P. Y.; Xu, B. Y.; Li, X. L.; Gao, F.; Zhai, J. G.; Wang, D. Y. Self-cleaning cotton fabrics with good flame retardancy *via* one-pot approach. *Polym. Degrad. Stabil.* **2021**, *192*, 109700.
45 Rao, W. H.; Tao, J.; Yang, F. H.; Wu, T.; Yu, C. B.; Zhao, H. B. Growth of copper organophosphate nanosheets on graphene oxide to improve fire safety and mechanical strength of epoxy resins. *Chemosphere* **2023**, *311*, 137047.
46 Niu, H. X.; Ding, H. L.; Huang, J. L.; Wang, X.; Song, L.; Hu, Y. A Furan-based phosphaphenanthrene-containing derivative as a highly efficient flame-retardant agent for epoxy thermosets without deteriorating thermomechanical performances. *Chinese J. Polym. Sci.* **2022**, *40*, 233–240.
47 Yu, C. B.; Wu, T.; Yang, F. H.; Wang, H.; Rao, W. H.; Zhao, H. B. Interfacial engineering to construct P-loaded hollow nanohybrids for flame-retardant and high-performance epoxy resins. *J. Colloid Interface Sci.* **2022**, *628*, 851–863.
48 Li, R. M.; Deng, C.; Deng, C. L.; Dong, L. P.; Di, H. W.; Wang, Y. Z. An efficient method to improve simultaneously the water resistance, flame retardancy and mechanical properties of POE intumescent flame-retardant systems. *RSC Adv.* **2015**, *5*, 16328–16339.
49 Wang, T. S.; Liu, T.; Ma, T. T.; Li, L. P.; Wang, Q. W.; Guo, C. G. Study on degradation of phosphorus and nitrogen composite UV-cured flame retardant coating on wood surface. *Prog. Org. Coatings* **2018**, *124*, 240–248.

https://doi.org/10.1007/s10118-024-3100-1